Demonstration of UWB Communication for Implants Using an Energy Detector

Mario Leib*, Thai Mach*, Bernd Schleicher†, Çağrı A. Ulusoy†, Wolfgang Menzel*, and Hermann Schumacher†

*Ulm University, Microwave Techniques, Albert-Einstein-Allee 41, 89081 Ulm, Germany
†Ulm University, Electron Devices and Circuits, Albert-Einstein-Allee 45, 89081 Ulm, Germany
Email: mario.leib@uni-ulm.de

***Abstract*—The communication with implants with high data rates is a demand for future medical devices. In this paper, the energy detector is evaluated as receiver concept for an IR-UWB communication system coping with data rates in the Mbit/s-range and the dispersive effects of human tissue. Beside the demonstration of a unidirectional transmission from a transmitter to a receiver within a tissue mimic liquid, the focus is on the system components, in particular on the squaring circuit.**

***Index Terms*—ultra-wideband (UWB), communication, impulse radio, biomedical telemetry, energy detection, on-off keying**

I. Introduction

The progress in medical technology leads to more and more sophisticated implanted devices for diverse applications. Cameras are integrated into capsules, which can be swallowed for endoscopy [1], cochlear implants are developed in order to stimulate hearing for deaf people [2] and retinal prostheses are applied to patients with certain eye diseases to achieve some ability to see [3]. In a more futuristic research project, the nerves of human beings are contacted, recorded, and transmitted outside of the human body. These data shall be used for smart prostheses [4]. For all of these mentioned medical devices, wireless data transmission with data rates of more than 10 Mbit/s are desired, whereas a low power consumption is mandatory for a long battery lifetime of the implants. The medical implant communication service (MICS) operating at 402 MHz–405 MHz cannot cope with these data rates as the MICS is limited to 800 kbit/s [5]. The ultra-wideband (UWB) technology operating from 3.1 GHz to 10.6 GHz can achieve much higher data rates and offers the ability of low-power consumption due to simple transmitter and receiver architectures of impulse-based radio (IR) systems.

For UWB-IR receivers, many different approaches are feasible. A correlation receiver acts like a matched filter, if properly synchronized and if the reference signals is identical to the received signal. Then the signal-to-noise ratio (SNR) is maximized and the receiver shows the best performance. However, the required precise synchronization is hardly realizable and the dispersive properties of human tissue lead to unpredictable shapes of the received signals. Non-coherent detectors are suboptimal, but are unsusceptible regarding dispersive effects of the channel, they do not need a precise synchronization and have an even more simple architecture leading to a lower power consumption. Hence, they are well-suited for communication with implants.

Non-coherent receiver concepts are the transmitted reference scheme or the energy detection. In the first case, two UWB impulses are transmitted for one data bit. The first impulse is unmodulated and used as reference, while the second one is delayed and modulated. In the receiver, these two impulses are multiplied using a power splitter, a delay line, and a mixer. In the energy detector, the same detection principle is applied, but with only one impulse and no delay. Hence, a self-mixing takes place. Both concepts have similar performance [6], but the energy detector is less complex as no delay line is needed. Furthermore, possible narrow-band interferer within the operating frequency band could be suppressed for the energy detector using the comb-filter approach described in [7]. This would improve the SNR additionally. Therefore, the energy detector has been chosen for the UWB-IR receiver in order to demonstrate the communication with implants. For the demonstration, on-off keying is used as modulation scheme and an unidirectional transmission with a data rate of 100 Mbit/s is chosen. This data rate and a unidirectional transmission is sufficient for all described medical applications.

II. Transmitter and Receiver Architecture

In Fig. 1 the block diagram of transmitter and receiver for the energy detector are depicted. The transmitter basically consists of a UWB impulse generator (IG) and an antenna. The transmit data itself is generated externally by a bit pattern generator, clocked by a signal generator.

The core element of the energy detector is the squaring device (SQR) transforming the received UWB impulses to

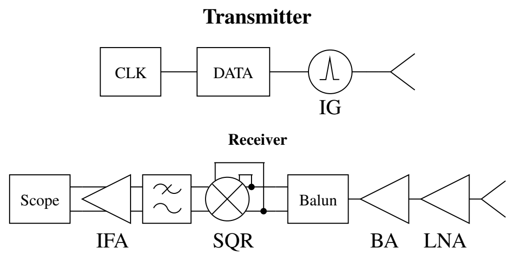

Fig. 1. Block diagram of the transmitter and the receiver.

base band. This signal is low-pass filtered, amplified (IFA), and displayed on an oscilloscope. For further signal processing in the digital domain, a comparator circuit with a properly adjusted threshold voltage can be applied. The receiver is dimensioned for a path attenuation of 50 dB, hence a UWB low-noise amplifier (LNA) and additional buffer amplifiers (BA) are required in order to operate the SQR with a suitable conversion loss. A UWB passive balun is used to combine the single-ended amplifier stages with the differential SQR.

For the BAs and the IFA, commercially available components have been used, although the specific BAs used here are not specified for the upper frequencies of the UWB range. However, this is tolerated by the energy detection concept. All self-designed active UWB components are described in more detail in the following section.

The power consumption of the individual components is listed in Table I. For the receiver, the overall power consumption is currently unacceptable for an implant and must be drastically reduced for each component. A sufficient value of 38 mW is achieved for the IG in the transmitter, which can be further decreased to the µW-range in a sleep-mode operation [8]. Therefore, at least a unidirectional transmission with an implanted transmitter, e. g. for neural recording or capsular endoscopy, is already practicable.

TABLE I
POWER CONSUMPTION OF ACTIVE COMPONENTS

IG	LNA	BAs	SQR	IFA
38 mW	55 mW	290 mW	66 mW	140 mW

III. PROPERTIES OF KEY COMPONENTS

A. Active Circuit Components

The realization of the transceiver system includes self-developed integrated circuits, which were all fabricated in the 0.8 µm Si/SiGe HBT technology from Telefunken Semiconductors. The used UWB impulse generator presented in [9] generates an FCC-compliant output waveform close to a fifth derivative Gaussian impulse with $\sigma = 51$ ps and a peak-to-peak amplitude of 520 mV. The UWB LNA has a gain of 23.5 dB and a noise figure of 2.8 dB–3.2 dB in the 3.1 GHz–10.6 GHz UWB band, as well as a 1 dB input compression point of -19.5 dBm at 7 GHz. For further information see [10].

The used fully differential squaring circuit consists of a four-quadrant multiplier and a predistortion input stage. A simplified circuit schematic can be seen in Fig. 2. The squaring operation can be considered as a multiplication of both input signals with each other. The multiplier is based on a double-balanced Gilbert cell multiplier, which operates all transistors in the linear region. To increase the linearity of the circuit, a resistive emitter degeneration is applied to the lower pair transistors of the Gilbert cell. The linearity of the upper four transistors are increased by a predistortion stage as suggested in [11].

The linearity of the squaring circuit can be read from the simulation of Fig. 3, where the differential DC output power

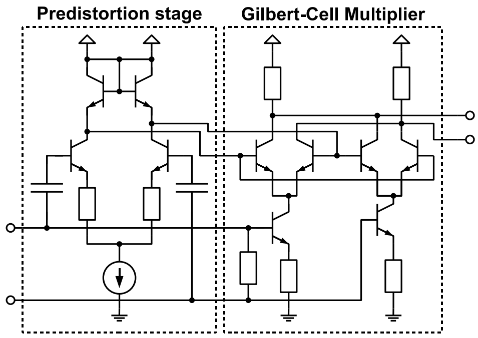

Fig. 2. Simplified schematic of the fully differential squaring circuit.

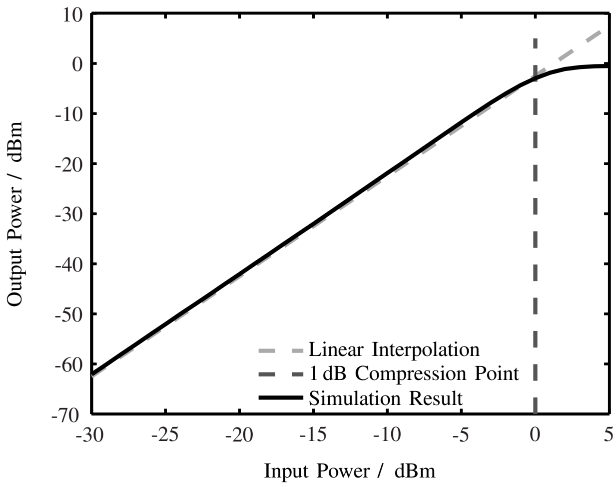

Fig. 3. Simulated output power of the squaring circuit at DC versus input power at 6.5 GHz.

is plotted versus the differential input power of a mid-band 6.5 GHz sinusoidal signal. The slope of the curve increases with 2 dBm/ dBm, which is the typical behavior for squaring. The simulated input 1 dB compression is 0 dBm.

An on-wafer time-domain evaluation of the circuit is performed. Therefore, the impulse generator is connected to a passive balun and differential probes are applied to an oscilloscope with 13 GHz measurement bandwidth. In Fig. 4 a comparison of the output waveform of the squaring circuit and the feeding impulse for the squaring IC is depicted. The input impulse is a slightly distorted version of the original fifth Gaussian derivative input impulse, which is originating from the attenuation and group delay variation of the UWB balun. The basic squaring operation is visible by the measured output signal, as a negligible amount of negative amplitudes are obtained. The squaring IC has a chip size of $440\,\mu m \times 460\,\mu m$ including pads.

B. UWB Antennas

Depending on the location of transmitter and receiver (implanted or outside), a UWB antenna designed for free space and for human tissue is required. For the implanted antenna, a UWB triplate-fed slot antenna optimized for radiation in

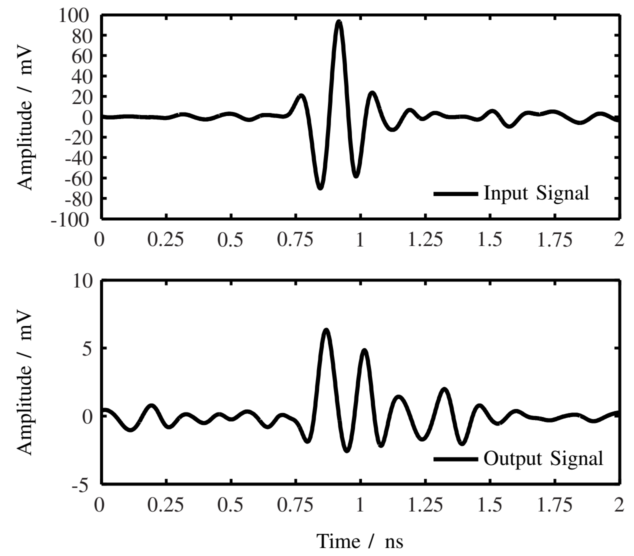

Fig. 4. Measured normalized time-domain output of the squaring circuit and the feeding impulse.

human tissue is used [12]. This antenna has a mean gain of 3.8 dBi within the UWB frequency range and can be immersed in a tissue mimic liquid. Hence, the communication with an implant can be simulated. For the antenna in free space, an available Vivaldi antenna [13] with a more directive radiation pattern and a mean gain of 7.2 dBi is applied.

IV. Evaluation of the Energy Detector

In order to evaluate the energy detector, the transmission of a UWB impulse is carried out with an ideal channel without any dispersive effects or influences of the antenna. A variable attenuator is connect therefore between the transmitter and the receiver. Fig. 5 shows the obtained output voltage swing for different path attenuations. At around 65 dB attenuation the noise floor is reached with the described setup.

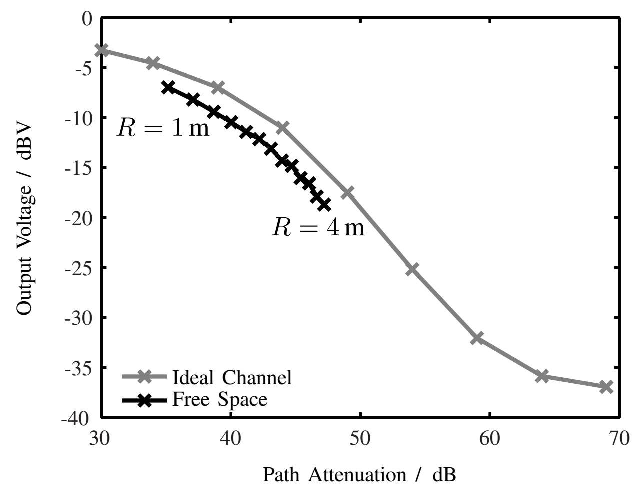

Fig. 5. Output voltage of the energy detector in case of the transmission of a UWB impulse for varying path attenuation.

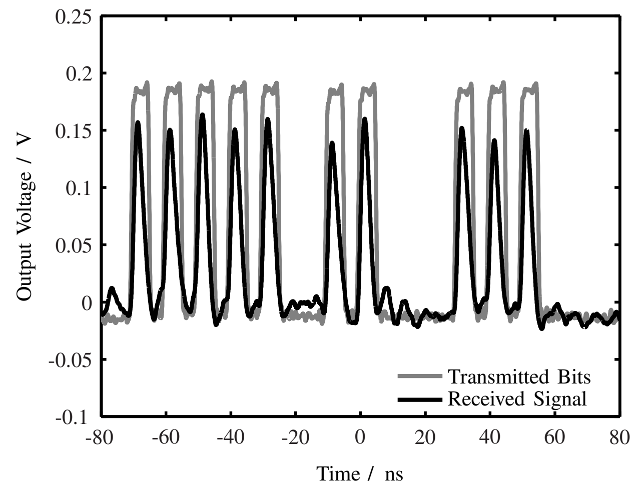

Fig. 6. Typical output signal of the receiver for the transmission of a UWB impulse in free space measured for a receiver distance of 4 m.

In a next step, the transmission in free space is performed for different distances R between transmitter and receiver using Vivaldi antennas. The output signal for a distance of 4 m is depicted in Fig. 6 for a certain bit pattern. As can be seen, the transmitted bits are recovered by the energy detector. The output voltage swing is displayed in Fig. 5 for the calculated path attenuation of each distance starting from 1 m in 0.5 m steps up to 4 m. The slight difference between the free space transmission and the ideal channel is caused by the applied approximations in order to calculate the path attenuation for a certain R using Friis transmission equation.

V. Communication in Tissue Mimic Liquid

To demonstrate the transmission in an environment similar to human tissue with a highly dispersive and lossy behavior, two antennas are immersed in a tissue mimic liquid. This liquid consists mainly of sugar and water. Its loss properties are shown in Fig. 7 in comparison to measured human skin and muscle tissue. The relative dielectric constant ε_r of the liquid is similar to skin tissue and has a value of 28 at 7 GHz.

The influence of the dispersive behavior on the impulse shape is illustrated in Fig. 8. There, the output signal after the transmission within the phantom liquid is shown in comparison to the input signal. Due to increased losses for higher frequencies, the impulse shape is significantly broadened and the amplitude is decreased by approximately 60 dB for the used path distance of 23.5 mm between two immersed antennas. A data transmission is still achievable in this cases as illustrated by the reception of a typical bit pattern in Fig. 9. To this end, an additional amplifier with 12 dB gain is inserted after the impulse generator in order to compensate for the high losses. This measurement setup demonstrates the transmission from a deeply implanted device to a reading device placed directly on the human body, e. g. applicable for capsular endoscopy.

In a final scenario, the communication of a less deeply implanted device with a base station outside the human body

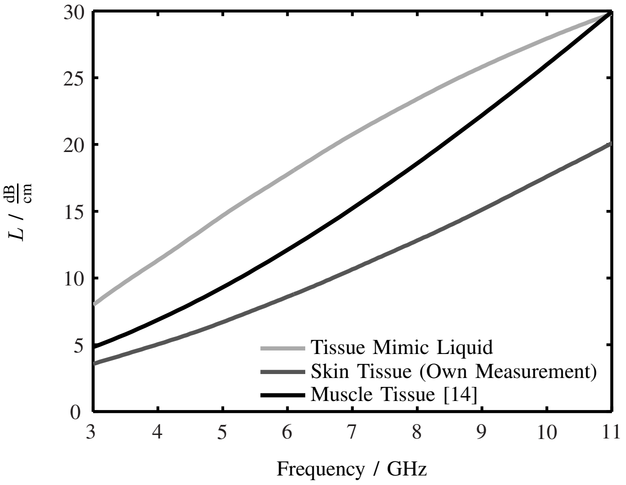

Fig. 7. Attenuation per unit length L of the tissue mimic liquid and some human tissues.

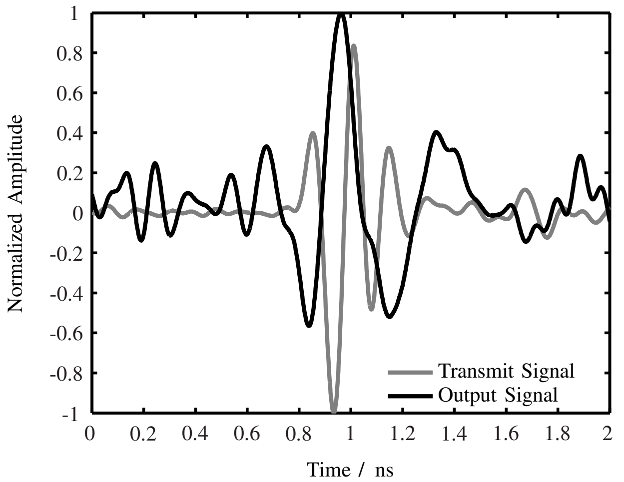

Fig. 8. Normalized output signal for the transmission of a UWB impulse in the phantom liquid directly after the receive antenna and transmit signal.

is considered. There, one antenna is immersed in the phantom liquid and a second one is located outside in free space. In this setup, the distance of the immersed antenna to free space is fixed to 15 mm, and the location of the outer antenna is varied. Similar measurement results are obtained thereby as before. The observed maximum distance of the base station for a reception is 15 cm, then the attenuation limit is reached.

VI. Conclusion

In this paper it is shown practically that the energy detector is a suitable receiver concept for the UWB communication with implants. Measurements are performed with a data rate of 100 Mbit/s meeting the requirements for modern medical devices.

Acknowledgment

The authors would like to thank Telefunken Semiconductors, Heilbronn, Germany, for the fabrication of the ICs and

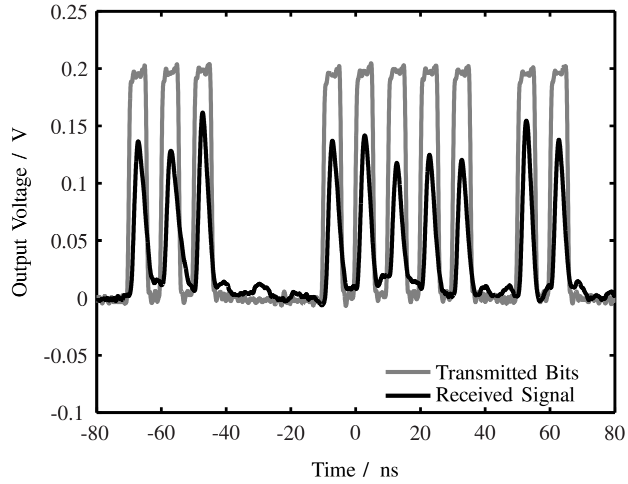

Fig. 9. Typical output signal of the receiver for the transmission of a UWB impulse in a dispersive human tissue phantom liquid, measured for a receiver distance of 23.5 mm.

the German research foundation (DFG) for funding the work by means of the priority program UKoLoS.

References

[1] T. Dissanayake, M. R. Yuce, and C. Ho, "Design and evaluation of a compact antenna for implant-to-air UWB communication," in *IEEE Antennas Wireless Propagat. Lett.*, vol. 8, Jul. 2009, pp. 153–156.

[2] T. Buchegger, G. Oßberger, A. Reisenzahn, E. Hochmaier, A. Stelzer, and A. Springer, "Ultra-wideband transceivers for cochlear implants," *EURASIP Journ. Appl. Sig. Process.*, vol. 18, pp. 3069–3075, Jan. 2005.

[3] K. Gosalia, G. Lazzi, and M. Humayun, "Investigation of a microwave data telemetry link for a retinal prosthesis," *IEEE Trans. Microwave Theory Tech.*, vol. 52, no. 8-2, pp. 1925–1933, Aug. 2004.

[4] M. R. Yuce, H. C. Keong, and M. S. Chae, "Wideband communication for implantable and wearable systems," *IEEE Trans. Microwave Theory Tech.*, vol. 57, no. 10, pp. 2597–2604, Oct. 2009.

[5] P. Bradley, "An ultra low power, high performance medical implant communication system (MICS) transceiver for implantable devices," in *IEEE Biomedical Circuits a. Systems Conf.*, Nov. 2006, pp. 158–161.

[6] L. Stoica, "Non-coherent energy detection transceivers for ultra wideband impulse radio systems," Dissertation, University of Oulu, 2008.

[7] T. Thiasiriphet and J. Lindner, "A novel comb filter based receiver with energy detection for UWB wireless body area networks," in *IEEE Intern. Wireless Comm. Systems Symp.*, Oct. 2008, pp. 498–502.

[8] B. Schleicher, J. Dederer, and H. Schumacher, "Si/SiGe HBT UWB impulse generators with sleep-mode targeting the FCC masks," in *IEEE Intern. Ultra-Wideband Conf. (ICUWB)*, Sep. 2009, pp. 674–678.

[9] J. Dederer, B. Schleicher, F. A. T. Santos, A. Trasser, and H. Schumacher, "FCC compliant 3.1-10.6 GHz UWB pulse radar using correlation detection," in *IEEE Intern. Microwave Theory a. Techniques Symp.*, Jun. 2007, pp. 1471–1474.

[10] J. Dederer, A. Trasser, and H. Schumacher, "Compact SiGe HBT low noise amplifiers for 3.1-10.6 GHz ultra-wideband applications," in *Topical Meeting on Silicon Monolithic Integrated Circuits in RF Systems*, Jan. 2006, pp. 391–394.

[11] P. R. Gray, P. J. Hurst, S. H. Lewis, and R. G. Mayer, *Analysis and Design of Analog Integrated Circuits*, 4th ed. John Wiley & Sons, Inc., 2001.

[12] M. Leib, M. Frei, D. Sailer, and W. Menzel, "Design and characterization of a UWB slot antenna optimized for radiation in human tissue," in *IEEE Intern. Ultra-Wideband Conf. (ICUWB)*, Sep. 2009.

[13] P. Gibson, "The Vivaldi aerial," in *European Microwave Conf. (EuMC)*, Oct. 1979, pp. 101–105.

[14] S. Gabriel, R. W. Lau, and C. Gabriel, "The dielectric properties of biological tissues: III. parametric models for the dielectric spectrum of tissues," *Phys. Med. Biol.*, vol. 41, no. 11, pp. 2271–2293, Nov. 1996.